Bulletin of the Seismological Society of America, Vol. 96, No. 2, pp. 456–466, April 2006, doi: 10.1785/0120050089

Unbiased Moment-Rate Spectra and Absolute Site Effects in the Kachchh Basin, India, from the Analysis of the Aftershocks of the 2001 M_w 7.6 Bhuj Earthquake

by Luca Malagnini, Paul Bodin, Kevin Mayeda, and Aybige Akinci

Abstract What can be learned about absolute site effects on ground motions, with no geotechnical information available, in a very poorly instrumented region? In addition, can reliable source spectra be computed at a temporary deployment? These challenges motivated our current study of aftershocks of the 2001 M_w 7.6 Bhuj earthquake, in western India, where we decouple the ambiguity between absolute source radiation and site effects by first computing robust estimates of coda-derived moment-rate spectra of about 200 aftershocks in each of two depth ranges. Crustal attenuation and spreading relationships, based on the same data used here, were determined in an an earlier study.

Using our new estimates of source spectra, and our understanding of regional wave propagation, for direct *S* waves we isolate the absolute site terms for the stations of the temporary deployment. Absolute site terms for each station were determined in an average sense for the three components of the ground motion via an L_1-norm minimization. Results for each site were averaged over wide ranges of azimuths and incidence angles.

The Bhuj deployment is characterized by a variable shallow geology, mostly of soft sedimentary units. Vertical site terms in the region were observed to be almost featureless (i.e., flat), with amplifications slightly <1.0 within wide frequency ranges. As a result, the horizontal-to-vertical (H/V) spectral ratios observed at the deployment mimic the behavior of the corresponding absolute horizontal site terms, and they generally overpredict them. This differs significantly from results for sedimentary rock sites (limestone, dolomite) obtained by Malagnini *et al.* (2004) in northeastern Italy, where the H/V spectral ratios had little in common with the absolute horizontal site terms.

Spectral ratios between the vector sum of the computed horizontal site terms for the temporary deployment with respect to the same quantity computed at the hardest rock station available, BAC1, are seriously biased by its nonflat, nonunitary site response. This indicates that, occasionally, the actual behavior of a rock outcrop may be far from that of an ideal, reference site (Steidl *et al.*, 1996).

Introduction

Two challenges for seismologists involved in monitoring activities are the accurate estimates of earthquake source spectra and the quantification of the complicated and varying effects of wave propagation at each recording site (the "site effect"). Although it may not appear obvious in theory, these two problems are linked in practice. This is particularly true when we deal with earthquakes smaller than, say, $M_w \sim 3$, that are difficult to waveform model because their radiated seismic energy is dominantly at high frequencies, which suffer (relative to the generally modeled low frequencies) stronger attenuation, scattering, and distortion, much of this from site effects. So whereas "crustal" wave propagation from the earthquake source to the site in general is regarded as being well-behaved enough to be accounted for, there remains the problem of deciding which stable feature(s) of the recorded high-frequency seismogram represent(s) the imprint of the source and which one(s) was/were caused by variable site effects underneath the recording stations.

Both "ends" of the earthquake process, its source and the effect of local geology at the recording site, are important

but often for different seismological applications. Seismologists interested in reliable detection and determination of earthquake source parameters and understanding rupture processes will focus on the source problem, but those studying seismic hazards are, in general, concerned about site effects.

In this article we try to separate out these effects in an average sense—that is, we try to find parameters that best reproduce the ensemble features of a particular regional dataset. (One could, alternatively, try to model individual waveforms.) We use a dataset for which we earlier studied the average regional crustal propagation: aftershocks of the 2001 Bhuj, India, earthquake, in western India. Data were recorded on a temporary seismic network deployed in a poorly studied region. In this sense, our study also addresses another challenge: what can be usefully learned (from both the source and site perspective) from an opportunistic study of earthquakes in an otherwise poorly characterized region, at a collection of not-well-documented sites? In earlier studies of these data, Bodin and Horton (2004) located the earthquakes accurately, and Bodin *et al.* (2004) studied the average crustal attenuation and spreading functions. However, Bodin *et al.* (2004) did not attempt to determine site terms in an absolute sense, nor did they compute source spectra without making some assumptions about the site effects.

In this article we build on these earlier studies by employing an efficient and accurate method of determining moment-rate source spectra based on stable coda-derived spectral measurements (Mayeda and Walter, 1996; Mayeda *et al.*, 2003). This method yields moment-rate spectra unbiased by the distorting effects of the surface geology; it has been tested extensively in a variety of regions. We then isolate the site response after deconvolving (removing) the source spectrum from the direct *S*-wave spectra of the Bhuj aftershock data and accounting for crustal wave propagation using the parameters determined by Bodin *et al.* (2004). We interpret our results to explore several timely issues in earthquake source mechanics and near-site wave propagation, which we describe in the remainder of this introduction.

If the moment-rate spectra can be calibrated accurately in a wide frequency range, in particular, at frequencies above the source "corner frequency," it becomes possible to assess the radiated seismic energy, or, equivalently, the dynamic stress drop, of each event (Mayeda and Walter, 1996). Numerous studies have recently addressed the quantification of the seismic energy and/or of the dynamic stress drop (Kanamori and Heaton, 2000; Brodsky and Kanamori, 2001; Ide and Beroza, 2001; Malagnini *et al.*, 2004; Mayeda *et al.*, 2005a; Morasca *et al.*, 2005). These studies basically focused on the variations of the normalized radiated energy as a function of the earthquake size (moment magnitude) to yield macroscopic information on fundamental dynamic properties of fault rupture. Some studies (e.g., Kanamori and Heaton, 2000; Brodsky and Kanamori, 2001) proposed specific physical mechanisms as governing the energy budget during the rupture of a fault patch. The hypothesis that dynamic stress drop of earthquakes is independent of size is venerable and has recently been reiterated by Ide and Beroza (2001) and Prieto *et al.* (2004). However, many researchers propose that the dynamic stress drop increases with increasing magnitude (Mayeda and Walter, 1996; Kanamori and Heaton, 2000; Brodsky and Kanamori, 2001; Izutani and Kanamori, 2001; Richardson and Jordan, 2002; Venkataraman *et al.*, 2002; Malagnini *et al.*, 2004; Mayeda *et al.*, 2005a; Morasca *et al.*, 2005).

Turning our attention to site effects, whatever the specific form and scaling of the source spectra, if accurate absolute source moment-rate spectra exist and if we possess accurate measures of regional crustal propagation of direct waves, then we have the information necessary to estimate the absolute site effects for the stations that were used in both the source and the attenuation studies. For example, starting from unbiased source spectra of earthquakes recorded in the eastern Alps by the Friuli-Venezia Giulia Seismic Network (FVGSN) and using the empirically determined regional wave propagation parameters in the eastern Alps (Malagnini *et al.*, 2002), Malagnini *et al.* (2004) estimated the absolute site effects of the FVGSN seismic stations. In the present study we followed procedures similar to Malagnini *et al.* (2004) to obtain the absolute source and site effects in the Kachchh Basin, India, using the aftershocks of the 2001 M_w 7.6 Bhuj earthquake.

In the scientific literature of the past decade, site transfer functions have been obtained by computing, from recordings of earthquake-induced ground motions, either the standard spectral ratio (SSR) (Borcherdt, 1970; King and Tucker, 1984; Tucker and King, 1984; Field and Jacobs, 1993, 1995) to a reference station, or the horizontal-to-vertical spectral ratio (HVSR) (Nakamura, 1989, 2000; Lachet and Bard, 1994; Theodulidis *et al*., 1996; Mucciarelli, 1998; Mucciarelli and Monachesi, 1998; Mucciarelli and Gallipoli, 2001). Given an ideal reference site (one with a flat absolute site response of unit amplitude) the SSRs yield accurate estimates of the absolute site terms.

The HVSRs may identify frequencies at which site effects may be important while not reliably quantifying absolute levels of spectral amplification or attenuation at a site. For example, Romanelli and Vaccari (1999) simulated the site response of the *SH* and *P-SV* motion in the town of Catania (see also, Panza *et al.*, 2001). Although the horizontal ground motions were strongly affected by the surface geology, the vertical motions were not. Their synthetic HVSRs, in agreement with observational results of other scientists (e.g., Lachet and Bard, 1994; Theodulidis *et al.*, 1996), clearly identified the resonance frequencies of sites but did not predict of their absolute amplitudes.

Although azimuthal variations are thought to be important in defining different site behaviors (see, for example, Papageorgiou and Aki, 1983), only 1D attenuation functions are used in this study, and no attempts are made to investigate azimuthally varying properties of sites. Because many trade-offs exist between the different variables that are spe-

cific for each site, estimating the absolute site terms of real seismic stations is challenging, and any estimate may depend on the specific choices of the different ingredients used. For example, in this study we use a function for crustal attenuation and spreading that is an average over azimuth and ray takeoff angles, and thus we can only obtain azimuth- and incidence angle-averaged "absolute" site terms. Nevertheless, we recognize that site effects may be strongly azimuth dependent, which probably contributes to the dispersion in our regression results.

The Bhuj Sequence Data Sets

The data used in this study were recorded by a network of eight portable seismographs deployed for 3 weeks, between 12 and 28 February 2001, starting 17 days after the 26 January 2001 Bhuj earthquake, M_w 7.6 (Bodin and Horton, 2004). The network recorded aftershocks as shallow as 5 km and extending to 35 km, or nearly through the presumed 40-km-thick crust. The strongest concentration of earthquakes is observed in the lower crust, at depths around 26 km (Bodin and Horton, 2004).

Bodin *et al.* (2004) selected two partially overlapping subsets of these events (860 shallow events, $H \leq 25$ km, and 535 deeper events, $H \geq 20$ km), and obtained a function describing the frequency-dependent crustal attenuation for seismic waves in the region. They observed slightly different apparent geometrical spreading and frequency dependence for the crustal parameter $Q(f) = Q_0(f/1.0)^{\eta}$ in the two cases. For both datasets $Q_{0\text{Shallow}} = Q_{0\text{Deep}} = 790$, whereas $\eta_{\text{Shallow}} = 0.22$, and $\eta_{\text{Deep}} = 0.35$. Moreover, the distribution of the stress parameter of the source spectra for the two datasets showed substantial differences in its dependence on the earthquake magnitude (Bodin *et al.*, 2004, their figure 8).

For this study, we selected two smaller subsets of seismic data from the deep and shallow ones defined by Bodin *et al.* (2004). We based our choice on their estimates of moment magnitude, obtained using the parameters of their crustal attenuation. We selected 981 observed waveforms from 174 events of $M_w > 2.7$ from the shallower data set, and 1808 observed waveforms from 215 deeper earthquakes of $M_w > 2.5$. This choice was not *a priori*, but rather selected after an initial analysis yielded noisy results when smaller earthquakes were included. Figures 1 and 2 shows maps and depth distributions of the two resulting subsets and their relationship to the seismic stations. The largest earthquake in the dataset was M_w 5.2, for an event common to both sets.

Data Analysis

We obtained unbiased moment-rate spectra for the two subsets of seismic data by analyzing the *S*-coda waves in different frequency bands, and tying these to estimates of the scalar seismic moments derived from waveform modeling of the larger events in the dataset. Moment-rate spectra were computed at a set of central frequencies that was

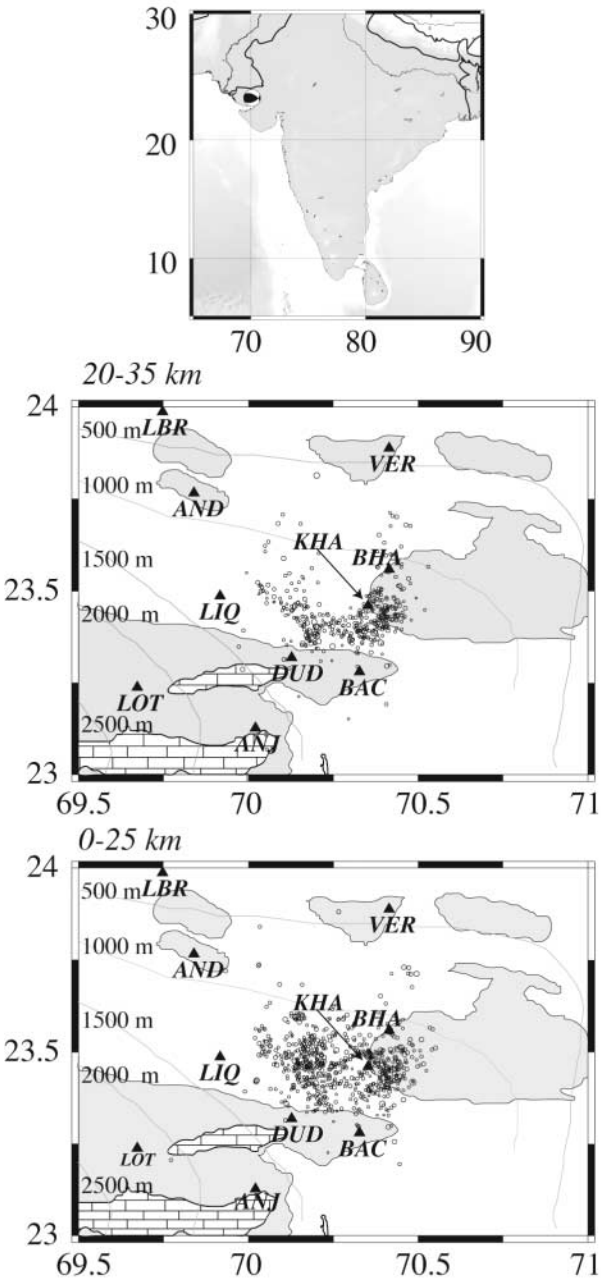

Figure 1. Maps of the region, showing earthquake epicenters of the events studied, locations and station codes of the three-component stations used, and generalized regional geology (according to Biswas, 1980). White backgrounds indicate areas of Quaternary outcrop, blocked fill patterns represent Cretaceous-aged outcrops, and gray is Jurassic sediments. Depth contours are labeled (in meters) with depth to Archean granite basement. The top frame shows a map of the Indian subcontinent, with the focal mechanism of the Bhuj mainshock indicating the area described by the two maps below. The middle frame is relative to the events of the "shallow" dataset (981 observed waveforms from 174 events occurred within 25 km from the free surface, with magnitude $M_w > 2.7$), and the bottom map describes the events of the "deep" dataset (1808 observed waveforms from 215 earthquakes deeper than 20 km, with magnitude $M_w > 2.5$).

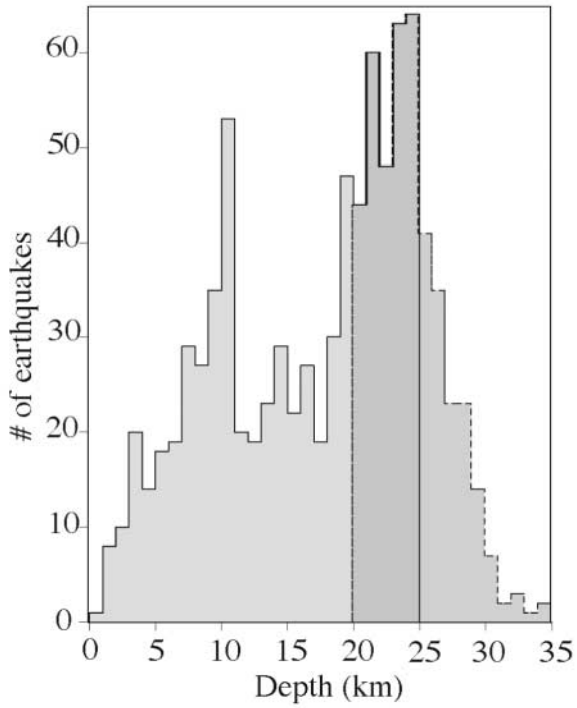

Figure 2. Histogram of the depth distributions of the aftershocks shown in Figure 1. The depth ranges of the two different datasets (deep and shallow) overlap between 20 and 25 km.

slightly different from that by Bodin *et al.* (2004) and subsequently resampled to match the central frequencies in their study. Before resampling, moment-rate spectra are transformed in ground velocity Fourier amplitudes.

Results from Bodin *et al.* (2004) are used to "propagate" the resampled moment-rate spectra to the arbitrary hypocentral distance of 40 km. After the regional propagation is achieved, the technique used in Raoof *et al.* (1999), Malagnini *et al.* (2000, 2002), Akinci *et al.* (2001), and Bodin *et al.* (2004) is applied to the Fourier amplitudes of the recorded earthquakes. An individual regression is run on the Fourier amplitudes observed for each sampling frequency, and the absolute site terms of each component of the ground motion of each one of the seismic stations are obtained.

Obtaining Absolute Moment-Rate Source Spectra

Obtaining the average source spectrum from the direct waves typically requires either some *a priori* information on the source mechanism or the availability of multiple stations to average out the source heterogeneities (e.g., source mechanism and directivity). In addition, path and site corrections can be significant, contributing to increased error in the final source spectrum. To minimize these effects we have used the coda methodology outlined in Mayeda *et al.* (2003) to derive stable source spectra. This methodology has been shown to provide the lowest variance estimate of the source spectrum in several tectonically diverse regions. We show in Figure 3 that the distance-corrected coda amplitudes have roughly a factor of five times less scatter than direct wave estimates. This 1D methodology has been applied to local and regional distances and appears to be well suited for small-scale studies (see, for example, the recent attenuation tomography of northern California by Mayeda *et al.*, 2005b). Because the coda envelope amplitudes are relative measures, we tie the long-period values to independently derived estimates from long-period waveform modeling (Fig. 4). This approach accounts for the *S*-to-coda transfer function and site effect corrections for frequencies below ~1.0-Hz. For the higher frequencies, we use several very small events as empirical Green's functions. Figure 5 shows representative coda-derived moment-rate spectra in units of dyne cm. Notice that independent of distance or azimuth, the individual station spectra are very similar, confirming that our calibration procedure is correct and demonstrating that the coda is not as sensitive to radiation pattern effects. All corrections were applied to the rest of the dataset to form source spectra. For additional stability, we formed the average spectra.

Absolute Site Terms

Let $a_k(r_{ij}, f)$ be the rms average of the *S*-wave Fourier spectral amplitudes, in the frequency window: $[f/\sqrt{2},\ \sqrt{2}\,f]$, observed on the *k*th waveform, at the *j*th site and during the *i*th event, at the hypocentral distance r_{ij}. We can write:

$$A_k(r_{ij}, f) = \mathrm{EXC}_j(r = r_{\mathrm{ref}}, f) + \mathrm{SITE}_i(f) + D(r_{ij}, r_{\mathrm{ref}}, f), \quad (1)$$

where

$$A_k(r_{ij}, f) = \log\left(a_k(r_{ij}, f)\right). \quad (2)$$

The time window used to isolate the specific spectral amplitudes starts 2 sec before the *S*-wave onset and has duration (past the *S*-wave arrival time) given by the time window containing the 5% to 75% of the seismic energy that follows the *S*-wave onset. For a clear description of the duration function, see Raoof *et al.* (1999) and Malagnini *et al.* (2002, 2004). The length of this time window is automatically computed on each filtered seismogram at each central frequency. This time window contains most of the direct *S* wave, or of the *Lg* wavetrain at the largest distances in the data set.

Using equation (1), we can cast all our observations in a matrix form and invert for the site terms: $\mathrm{SITE}_i(f)$, fixing the attenuation term, $D(r_{ij}, r_{\mathrm{ref}}, f)$, and all the excitation terms, $\mathrm{EXC}_j(r = r_{\mathrm{ref}}, f)$. The empirical attenuation terms are taken from the study by Bodin *et al.* (2004), for both the deep and the shallow data sets. The attenuation terms for the Fourier amplitudes at all the individual central frequencies are shown in Figure 6, whereas the excitation terms are obtained from the absolute moment-rate spectra described in the preceding section. The spectra are transformed to ground-velocity Fourier amplitudes and "propagated" to the

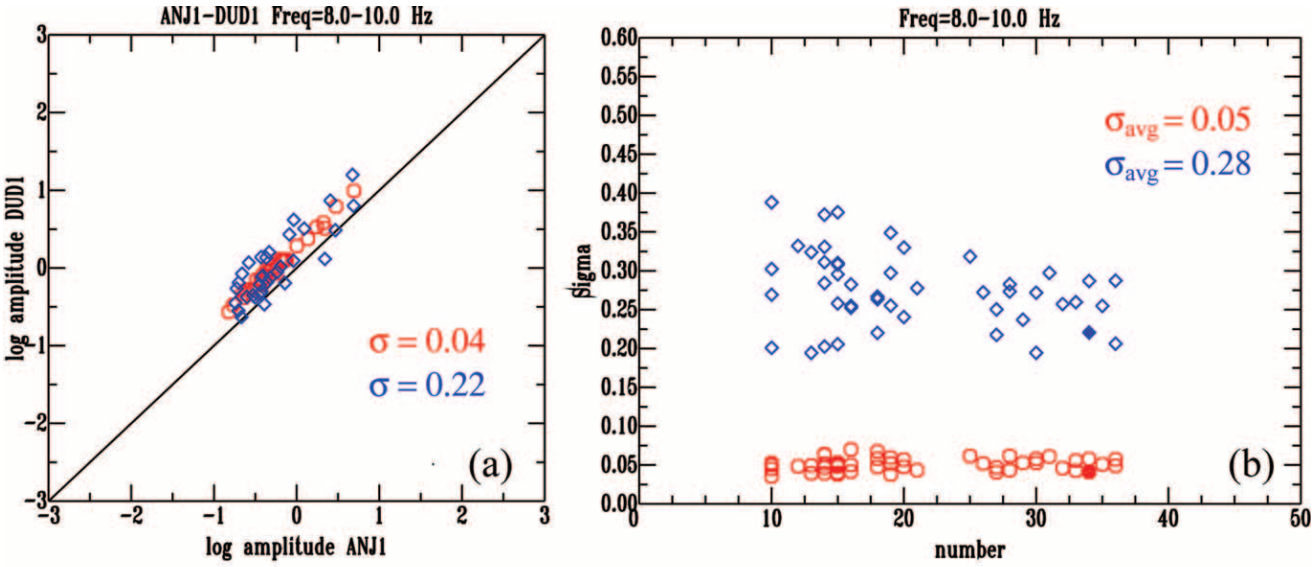

Figure 3. (Left) interstation scatter plot between stations DUD1 and ANJ1, in the frequency range between 8.0 and 10.0 Hz, obtained by plotting the distance-corrected coda spectral measurements (red symbols) and the distance-corrected direct-wave amplitudes (blue symbols). Note the large variance reduction when coda measurements are used. Direct-wave measurements are corrected for distance using the functional form provided by Bodin *et al.* (2004). DC offsets represent the interstation site effect. (Right) Summary plot for over 55 pairs of stations in the 8.0- to 10.0-Hz hand: the *x* axis represents the number of common events for each station pair, and the *y* axis is the data standard deviation. We also show the data point of the figure in the left frame as filled symbols in the frame on the right. Note that the average amplitude scatter is more than five times smaller for the coda.

reference distance r_{ref} = 40 km by using equations (3) and (9–12) from Bodin *et al.* (2004).

Table 1 from Bodin and Horton (2004) gives the available information about the eight seismic stations used in this study. As stated in their article, "Most stations were sited on rock (sandstone or basalt) or on a thin layer of soil overlying rock. LIQ is a notable exception. . . ." However, we point out that no geotechnical studies have been done at any of these sites and the geological mapping available is at a reconnaissance scale. For example, station BAC (Fig. 1) is on a small outcrop of Cretaceous-aged Deccan Trap basalt flow, overlooked in the geological map that forms the basis for the regional geology sketched in the figure.

Results

Site Effects in an Absolute Sense

In the following we describe the characteristics of each of the seismic stations' absolute site terms and of their known or inferred geological features. It is believed that strong-motion recordings are strongly affected by the local geology, in the shallowest 30 m (Anderson *et al.*, 1996). Figures 7 and 8 show the absolute vertical and horizontal site effects, and the H/V spectral ratios (HVSR) for the direct *S*-waves for all stations and form the basis for this discussion.

Station ANJ1, located on a sandstone formation, is characterized by amplification of the horizontal ground motions over the entire frequency range studied (1–12 Hz). Both the horizontal and vertical site terms are almost featureless (i.e., no discernible peaks, notches, or trends). The corresponding HVSR shows a positive trend, up to 8 Hz, where this quantity approaches a value of about 5.

Station BAC1, which we initially considered a good candidate for a "reference" rock site because it was directly on a basalt flow, shows a slight amplification of the horizontal ground motions at about 2 Hz and a strong deamplification at high frequencies (above 5 Hz). These features would result in a substantial bias of the interstation spectral ratios, because they will be amplified at high frequency due to the strong attenuation at shallow depths beneath site BAC1. A similar trend characterizes the vertical site term of this station and results in an almost flat HVSR, up to about 8 Hz. This quantity also shows a fast decrease at high frequency. Results relative to site BAC1 (Fig. 9) are consistent with the conclusions by Steidl *et al.* (1996), who showed that the site response of surface rock is not spectrally flat due to attenuation and scattering from near-surface weathering and cracking of the rocks.

The estimate of the absolute response of station BHA1, although deployed over deeply weathered sandstone, is very similar to that of station BAC1. The HVSR at this station is

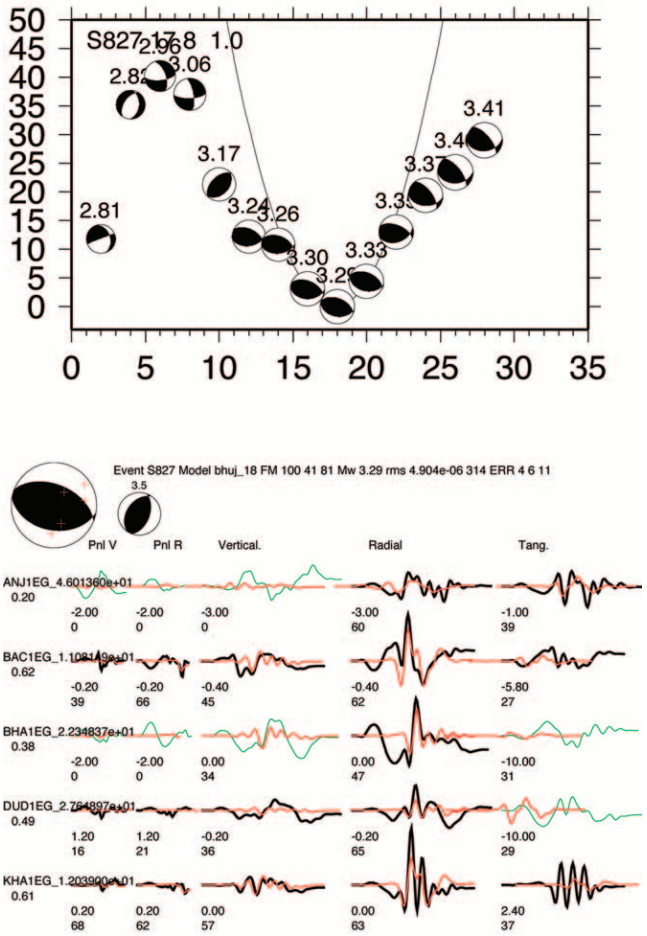

Figure 4. Waveform modeling of one of the calibration events. (Top) Misfit (normalized) as a function of centroid depth. In the figure are shown the best mechanisms of every point of the grid search on source depth. The method of Zhao and Helmberger (1994), further improved by Zhu and Helmberger (1996), was used to obtain this solution. (Bottom) Waveform fit: red seismograms are synthetic data, computed using the minimum misfit focal mechanism. Black seismograms are the observed data used in the inversion. Green seismograms are observed data inverted with zero weight.

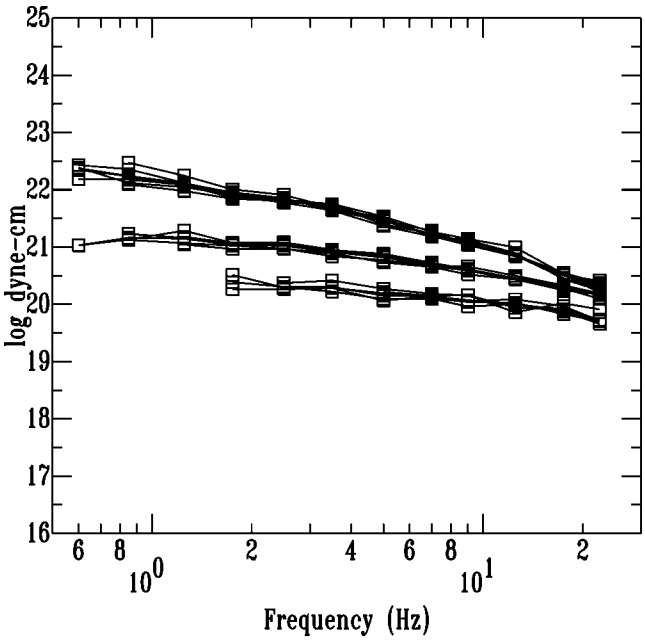

Figure 5. Individual moment-rate spectra computed for three events, each one at a specific set of recording stations. Note, for each event, how small the scatter of the spectral amplitudes is.

almost flat in the entire frequency band available and has the lowest absolute value.

Station DUD1 was the "best-behaved" station in the dataset. Its response is roughly flat and close to unity for the horizontal ground motion. The same behavior is observed on the vertical transfer function, and the HVSR for this station is almost featureless and low in amplitude. The station was deployed on the ground of a small (1-story) structure upon a soil layer of unknown thickness (Bodin and Horton, 2004).

Station KHA1 was deployed over a thin layer of soil of unknown thickness, overlying deeply weathered sandstone (Bodin and Horton, 2004). Some of the unusual characteristics of this site, compared with others in the network, may reflect that it was located on the floor of a cellar about 2 m below the surrounding ground surface. This station is characterized by a slight, broadband amplification of the horizontal ground motions, between 1 and 8 Hz. Amplification of the horizontal site term is sharply terminated at the higher frequencies. The vertical site effect at this station is relatively high between 1 and 2 Hz and then decays to a low level. The HVSR at this station mimics the horizontal site term.

Station LBR1, together with KHA1 and LIQ1, reveals the largest variations in the HVSR. The horizontal site term is characterized by a large amplification between 5 and 12 Hz. The vertical site term is flat and very low in amplitude. The HVSR reproduces the horizontal site term. The surface geology at LBR1 is characterized by the presence of slightly indurated sediments, cropping out on a bluff several meters high above the surrounding Great Rann of Kachchh.

Station LIQ1 shows a broadband amplification of horizontal ground motions at frequencies between 1 and 5 Hz. The trend at high frequency, observed on both the vertical and the horizontal ground motions, indicates a strong deamplification. The HVSR at this station is consistent with the observed horizontal site term. In the immediate vicinities of this station, extensive liquefaction phenomena were induced by the Bhuj mainshock. LIQ1 was intentionally located at the site of a large sand blow, where the thickness of unconsolidated sediments is thought to be around 500 m (Bodin and Horton, 2004).

Station LOT1 experiences amplification between 2 and 8 Hz in the horizontal absolute site term. At higher frequencies, the amplitudes of the horizontal site term decrease

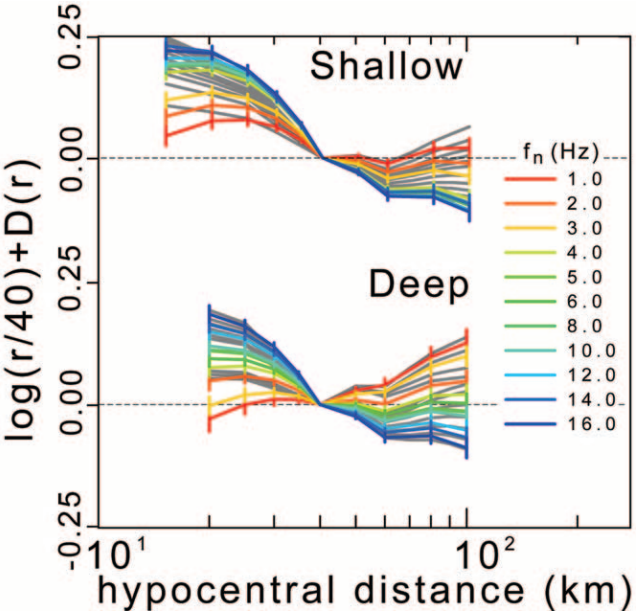

Figure 6. Empirical functions describing the regional attenuation for the shallow and deep bandpass-filtered peak ground motion (from Bodin *et al.*, 2004). Attenuation curves are normalized to $1/r$ (horizontal lines represent a $1/r$ decay of the filtered peak ground motion). Curves in color represent the empirical attenuation, whereas the gray curves in the background are theoretical predictions based on Random Vibration Theory, given a geometrical spreading function, a crustal parameter $Q = Q(f)$, and an empirical function describing the frequency-dependent duration of the ground motion as a function of hypocentral distance. Deep and shallow datasets are characterized by different attenuation features because the radiated energy in the two cases samples the crust in a different way.

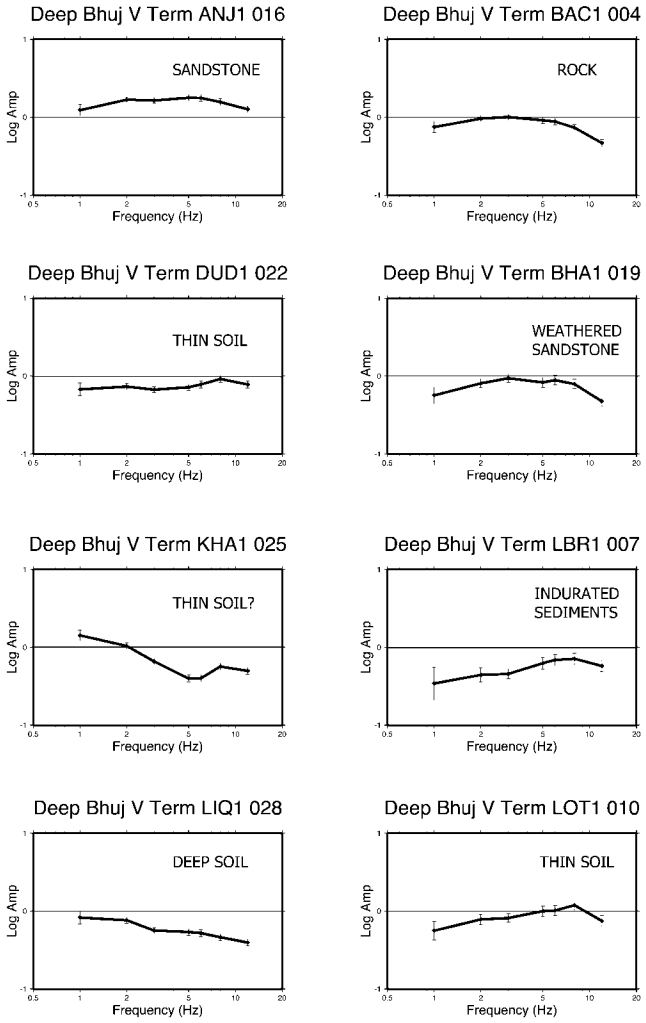

Figure 7. Vertical absolute site terms for the stations of the Bhuj temporary deployment. Error bars represent $\pm\ \sigma$. The terms shown in these frames were computed from the deep earthquakes dataset.

strongly. The vertical term at LOT1 is smooth, with a sharp peak at 8 Hz. The HVSR for this station shows a slight amplification with a relatively broad maximum between 5 and 8 Hz. At station LOT1, a thin soil layer overlies sandstone bedrock.

Differences between Deep and Shallow Datasets

Differences between site terms of the same stations, obtained by regressing the two different datasets are within the error bars of each term (Fig. 10). For this reason, we have discussed only the site terms derived from the deeper set of earthquakes. Note, however, that the regional attenuation obtained by Bodin *et al.* (2004) for the two sets of data differed, undoubtedly because seismic waves in the two cases would sample the regional structure slightly differently. It is a comforting "reality check" that the site terms we compute from two different datasets are so similar, because one would expect site terms to be (to first order) independent of the path taken to the site. This confirms our argument that, for the frequency band investigated in this study, the terms shown in Figures 7 and 8 reveal the absolute responses (in an average sense) of the very shallow geologic formations. Variations among the incidence angles of observed seismic waves, although they must contribute to the dispersion of the observations, do not seem to cause clear first-order systematic effects in the analyses.

H/V Spectral Ratios: Differences from the Results by Malagnini *et al.* (2004)

Comparing the absolute horizontal site terms with their corresponding HVSRs (Fig. 8) reveals similar values for both measures at low frequency ($f < 5$ Hz). At higher frequencies, in general, the HVSRs overestimate the absolute site terms. We also conclude that, for the sites shown in the figure, the spectral shapes of the two measures are similar in

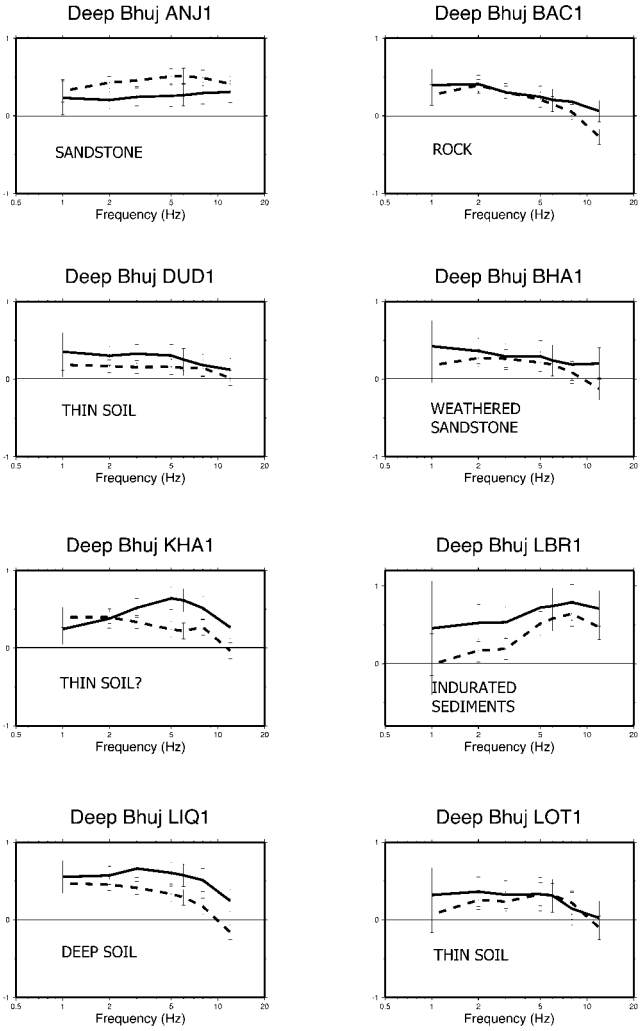

Figure 8. Horizontal absolute site terms and H/V spectral ratios for the deep Bhuj aftershocks. Dashed lines, horizontal absolute site terms (vector sum of the radial and the transverse individual site terms) for the stations of the Bhuj temporary deployment; solid lines, H/V ratios. Error bars represent $\pm\sigma$.

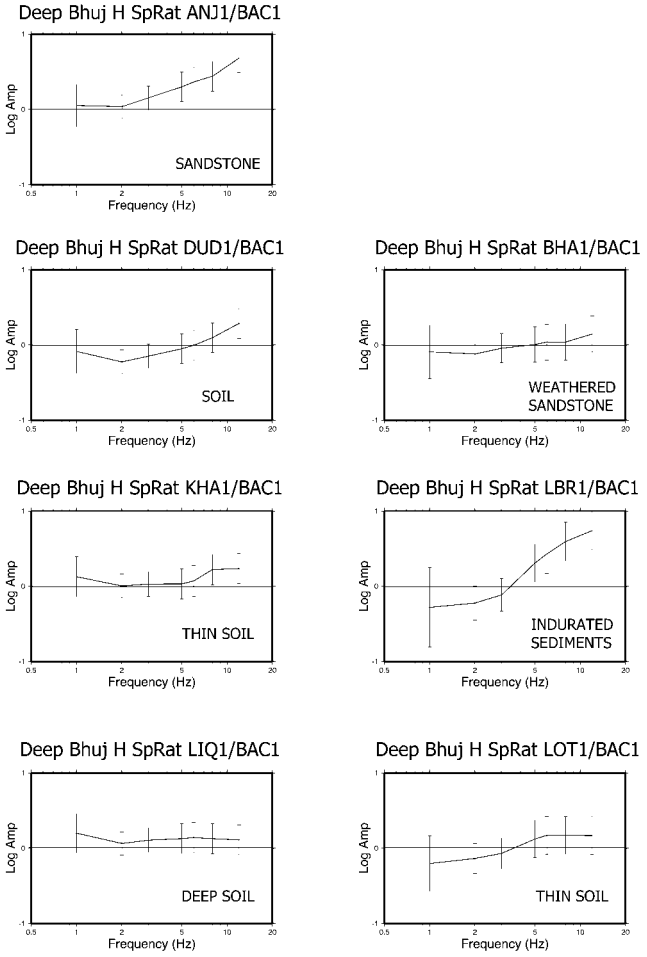

Figure 9. Spectral ratios between the absolute horizontal site terms (vector sum of the radial and the transverse site terms) of all stations to the horizontal absolute site term of station BAC1. Error bars represent $\pm\sigma$.

general. It is difficult to quantify these general remarks, given both the variability between stations and the uncertainties in the results.

The vertical absolute site terms (Fig. 7), are slightly less than unity over wide frequency ranges and do not show large variations. A notable exception is that of station KHA1, whose vertical absolute site term is characterized by a strong fall-off (almost a factor of 5) between 1 and 5 Hz.

Station ANJ1 (sandstone formation) shows the largest amplification, station LBR1 (slightly indurated sediments) is characterized by the lowest amplitudes at low frequency, and stations KHA1 (cellar-deployed on thin soil layer of unknown thickness) and LIQ1 (deployed over a large sand blow, unconsolidated deep soil) show the lowest amplitudes at high frequency ($f > 3$ Hz).

Discussions and Conclusions

In our study of Bhuj aftershocks the general pattern of absolute horizontal site terms at most stations is somewhat similar to their HVSRs. In the eastern Alps, Malagnini *et al.* (2004) demonstrated that rock sites revealed no clear relationships between the HVSRs and the corresponding absolute horizontal ground-motion transfer functions. They concluded that, although the HVSRs were strongly correlated with the site characteristics (geometry) and to the shallow geology, the hypothesis that the vertical motion is almost undisturbed, and that only the horizontal motion is strongly affected by the shallow geology, was in general incorrect.

Although the spectral shapes of the HVSRs and the absolute site terms for Bhuj earthquakes are similar in general the HVSRs do not successfully reproduce the absolute amplitudes of the amplification/resonance effects induced by the shallow geology, even at soil sites. In Bhuj, as well as

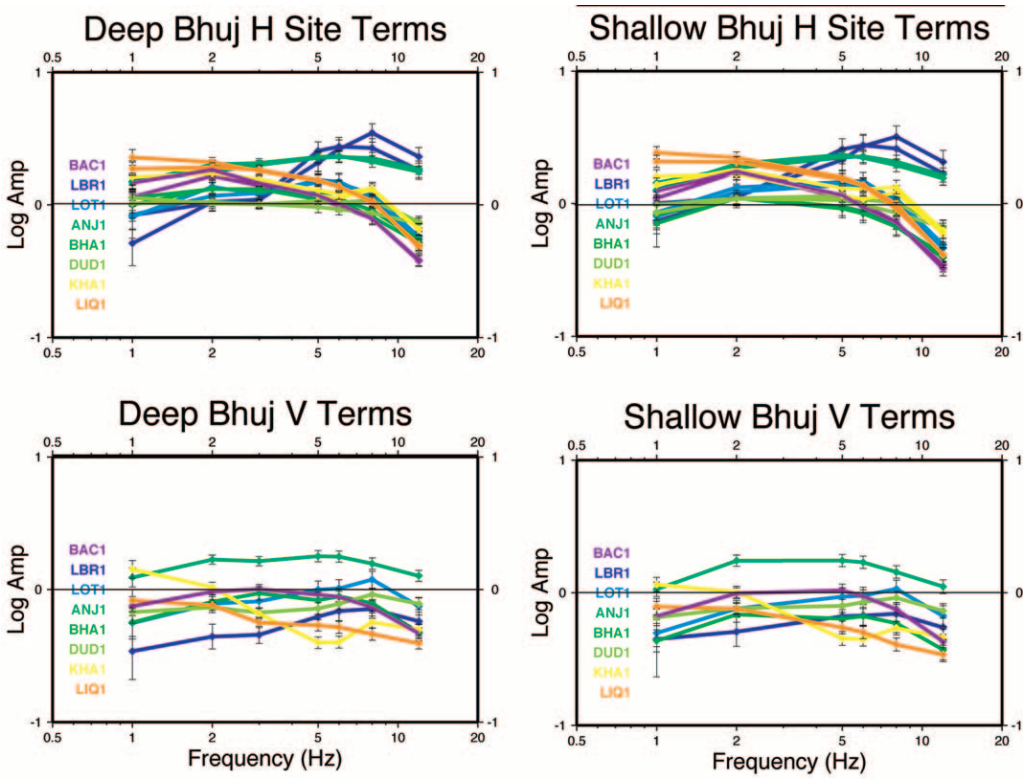

Figure 10. Absolute site terms obtained from the deep dataset (left frames), and from the shallow one (right frames). Upper frames show the individual horizontal terms (radial, transverse); lower frames show the vertical absolute site terms. The two sets of results are practically equivalent. Error bars represent $\pm\sigma$.

in the eastern Alps, our presumed "reference" rock site (station BAC1) is characterized by a strong deamplification of both the horizontal and the vertical ground motions. This result seems to be consistent with those by Malagnini *et al.* (2004). Unlike the results by Malagnini *et al.* (2004), the absolute horizontal site terms at station BAC1 are well reproduced by its HVSR.

Figure 9 shows the SSRs of all the horizontal absolute site terms of all stations with respect to BAC1. Each SSR is strongly biased by the deamplification effects at BAC1. The comparison between the SSRs (Fig. 9), the HVSRs, and the absolute horizontal site terms (Fig. 8), clearly shows that the SSRs to station BAC1 are the farthest from the actual absolute site terms.

At all sites in the present study, variations of the spectral shapes and amplitudes of the vertical site terms were only marginal. In other words, the amplitudes of the vertical site responses investigated in this study are smaller than the corresponding amplitudes of the horizontal site terms. Different sites, though, may have very different levels of vertical site response. This is not true universally, however for example, in the eastern Alps, Malagnini *et al.* (2004) determined for one site a strong deamplification at high frequency on both the horizontal and the vertical site transfer functions. Although the H/V ratio is strongly related to the shallow site geology and to the geometry of the buried units, it may not always describe the horizontal site transfer function. In this study, HVSRs show similar general trends in spectral shape and low-frequency amplitude as the horizontal motion transfer functions, although they overpredict them at most sites, at higher frequencies.

For both datasets, HVSRs describe the horizontal site transfer function (at least in terms of spectral shape, if not amplitude) better than interstation spectral ratios do. The latter may be biased by the nonflat, high-frequency response of rock sites.

Havenith *et al.* (2002) pointed out that SSRs and HVSRs were similar for the set of stations used in their article. Moreover, HVSRs were always lower or comparable to SSRs and were most consistent at frequencies lower than the fundamental resonance frequency. Beyond the resonance frequency, the HVSR may be considered as a lower bound of the corresponding SSR. In turn, the SSRs described in their article were up to a factor of 3 higher than the corresponding HVSRs. They also concluded that the investigated SSRs and HVSRs consistently indicated the same fundamental frequency at a specific site, with the HVSRs computed over different waves (direct *S*-waves, *S*-coda, noise) showing very stable spectral shapes.

We feel that the major drawback in our study is the

limited resolution in frequency on the "propagated" source spectra. This issue arises because two independent studies are needed to apply our regression: one on the ground-motion scaling, the second on the absolute source scaling. Although specific physical reasons not to use the same set of sampling frequencies do not exist, the same is not true for what concerns the bandwidths. On the one hand, beyond the event corner frequency, bandwidths must be very small because coda envelopes tend to be strongly dominated by signals in the lower side of the filtered band; on the other hand, the ground-motion studies need to rely on relatively large bandwidths to have meaningful and clear peak values.

Limited resolution in the 1- to 5-Hz frequency band does not allow us to see details in the absolute site spectra. The relatively large variability of the site terms at about 1.0 Hz suggests that the differences in the shallow geology can be large and can be responsible for the different site responses. At frequencies lower than 1.0 Hz, the results from the ground-motion study by Bodin *et al.* (2004) were unstable and are not used here.

The lack of resolution in the important (for structural engineers) frequency band between 1.0 and 5.0 Hz is mitigated by the strong averaging actions implicitly taken in the regressions (results would have been smooth anyhow). In fact, results are averaged over incidence and azimuth angles, and Herrmann and Malagnini (unpublished manuscript) demonstrated that variations in the two parameters may be responsible for the overall variability seen in their synthetic study.

Acknowledgments

This study was supported, in part, by project FIRB, Prot. RBAU013NRZ. Paul Bodin was funded by the U.S. Department of Energy under Cooperative Award DE-FC52-03NA9951 and by the Mid-America Earthquake Center through the Earthquake Engineering Research Centers Program of the National Science Foundation under NSF Award EEC-9701785. Work by K. Mayeda was performed under the auspices of the U.S. Department of Energy by the University of California, Lawrence Livermore National Laboratory under Contract W-7405-Eng-48. This is LLNL contribution UCRL-JRNL-211990.

Any opinions, findings and conclusions or recommendations expressed in this material are those of the authors and do not necessarily reflect those of the National Science Foundation or the U.S. Department of Energy. The authors are particularly grateful to Lupei Zhu and Robert B. Herrmann, for their help in the determination of the moment tensor solution of some of the small events used.

References

Akinci, A., L. Malagnini, R. B. Herrmann, N. A. Pino, L. Scognamiglio, and H. Eyidogan (2001). Predictive relationships for the ground motion in the Erzincan region (Turkey), *Bull. Seism. Soc. Am.* **91,** 1446–1455.

Anderson, J. G., Y. Lee, Y. Zeng, and S. Day (1996). Control of strong motion by the upper 30 m, *Bull. Seism. Soc. Am.* **86,** 1749–1759.

Biswas, S. K. (1980) Structure of Kutch-Kathiawar Region, W. India, in *Proc. 3rd Ind. Geol. Congr. Pune*, 255–272.

Bodin, P., and S. Horton (2004). Source parameters and tectonic implications of aftershocks of the M_w 7.6 Bhuj earthquake of January 26, 2001, *Bull. Seism. Soc. Am.* **94,** 818–827.

Bodin, P., L. Malagnini, and A. Akinci (2004). Ground-motion scaling in the Kachchh Basin, India, deduced from aftershocks of the 2001 M_w 7.6 Bhuj earthquake, *Bull. Seism. Soc. Am.* **94,** no. 5, 1658–1669.

Borcherdt, R. D. (1970). Effects of local geology on ground motion near San Francisco Bay, *Bull. Seism. Soc. Am.* **60,** 29–61.

Brodsky, E. E., and H. Kanamori (2001). Elastodynamic lubrication of faults, *J. Geophys. Res.* **106,** 16,357–16,374.

Field, E. H., and K. Jacob (1993). The theoretical response of sedimentary layers to ambient seismic noise, *Geophys. Res. Lett.* **20,** 2925–2928.

Field, E. H., and K. A. Jacob (1995). Comparison and test of various site-response estimation techniques including three that are not reference-site dependent, *Bull. Seism. Soc. Am.* **85,** 1127–1143.

Havenith, H.-B., D. Jongmans, E. Faccioli, K. Abdrakhmatov, and P.-Y. Bard (2002). Site effects analysis around the seismically induced Ananevo rockslide, Kyrgyzstan. *Bull. Seism. Soc. Am.* **92,** 3190–3209.

Ide, S., and G. C. Beroza (2001). Does apparent stress vary with earthquake size? *Geophys. Res. Lett.* **28,** 3349–3352.

Izutani, Y., and H. Kanamori (2001). Scale dependance of seismic energy-to-moment ratio for strike-slip earthquakes in Japan, *Geophys. Res. Lett.* **28,** 4007–4010.

Kanamori, H., and T. H. Heaton (2000). Microscopic and macroscopic physics of earthquakes, in *Geocomplexity and the Physics of Earthquakes*, J. Rundle, D. L. Turcotte, and W. Kein (Editors), American Geophysical Monograph 120, 147–155.

King, J. L., and E. Tucker (1984). Observed variations of earthquake motion across a sediment-filled valley, *Bull. Seism. Soc. Am.* **74,** 137–151.

Lachet, C., and P.-Y. Bard (1994). Numerical and theoretical investigations on the possibilities and limitations of the Nakamura's technique, *J. Phys. Earth* **42,** no. 4, 377–397.

Malagnini, L., A. Akinci, R. B. Herrmann, N. A. Pino, and L. Scognamiglio (2002). Characteristics of the ground motion in Friuli (Northeastern Italy), *Bull. Seism. Soc. Am.* **92,** 2186–2204.

Malagnini, L., R. B. Herrmann, and M. Di Bona (2000). Ground-motion scaling in the Apennines (Italy), *Bull. Seism. Soc. Am.* **90,** 1062–1081.

Malagnini, L., K. Mayeda, A. Akinci, and P. L. Bragat (2004). Estimating absolute site effects, *Bull. Seism. Soc. Am.* **94,** 1343–1352.

Mayeda, K., and W. R. Walter (1996). Moment, energy, stress drop, and source spectra of western United States earthquakes from regional coda envelopes, *J. Geophys. Res.* **101,** 11,195–11,208.

Mayeda, K., R. Gök, W. R. Walter, and A. Hofstetter (2005a). Evidence for non-constant energy/moment scaling from coda-derived source spectra, *Geophys. Res. Lett.* **32,** L10306, doi 10.1029/2005GL022405.

Mayeda, K., A. Hofstetter, J. L. O'Boyle, and W. R. Walter (2003). Stable and transportable regional magnitudes based on coda-derived moment-rate spectra, *Bull. Seism. Soc. Am.* **93,** 224–239.

Mayeda, K., L. Malagnini, W. S. Phillips, W. R. Walter, and D. Dreger (2005b). 2-D or not 2-D, that is the question: a northern California test, *Geophys. Res. Lett.* **32,** L12301, doi 10.1029/2005GL022882.

Morasca, P., K. Mayeda, L. Malagnini, and W. R. Walter (2005). Coda-derived source spectra, moment magnitudes and energy-moment scaling in the Western Alps, *Geophys. J. Int.* **160,** 263–275, doi 10.1111/j.1365-246X.2005.02491.x.

Mucciarelli, M. (1998). Reliability and applicability of Nakamura's technique using microtremors: an experimental approach, *J. Earthquake Eng.* **2,** 625–638.

Mucciarelli, M., and M. R. Gallipoli (2001). A critical review of 10 years of microtremor HVSR technique, *Boll. Geof. Teor. Appl.* **42,** 255–266.

Mucciarelli, M., and G. Monachesi (1998). A quick survey of local amplifications and their correlation with damage observed during the Umbro-Marchesan earthquake of September 26, 1997, *J. Earthquake Eng.* **2,** 325–337.

Nakamura, Y. (1989). A method for dynamic characteristics estimation of subsurface using microtremor on the ground surface, *Q. Rep. Rail. Tech. Res. Inst.* **30,** no. 1 25–33.

Nakamura, Y. (2000). Clear identification of fundamental idea of Nakamura's technique and its applications, in *Proc. 12th World Conference on Earthquake Engineering*, New Zealand, CD-Rom.

Panza, G. F., F. Romanelli, and F. Vaccari (2001). Seismic wave propagation in laterally heterogeneous anelastic media: theory and applications to seismic zonation, *Adv. Geophys.* **43,** 1–95.

Papageorgiou, A. S., and K. Aki (1983). A specific barrier model for the quantitative description of inhomogeneous faulting and the prediction of strong ground motion. Part II. Applications of the model, *Bull. Seism. Soc. Am.* **73,** 953–978.

Prieto, G., P. M. Shearer, F. L. Vernon, and D. Kilb (2004). Earthquake source scaling and self-similarity estimation from stacking P and S spectra, *J. Geophys. Res.* **109,** B08310, doi 10.1029/2004JB003084.

Raoof, M., R. B. Herrmann, and L. Malagnini (1999). Attenuation and excitation of three-component ground motion in Southern California, *Bull. Seism. Soc. Am.* **89,** 888–902.

Richardson, E., and T. H. Jordan (2002). Seismicity in deep gold mines of South Africa: implications for tectonic earthquakes, *Bull. Seism. Soc. Am.* **929,** 1766–1782.

Romanelli, F., and F. Vaccari (1999). Site response estimation and ground motion spectral scenario in the Catania Area, *J. Seism.* **3,** no. 3, 311–326.

Steidl, J. H., A. G. Tumarkin, and R. J. Archuleta (1996). What is a reference site? *Bull. Seism. Soc. Am.* **86,** 1733–1748.

Theodulidis, N., P.-Y. Bard, R. Archuleta, and M. Bouchon (1996). Horizontal to vertical ratio and geological conditions: the case of Garner Valley Downhole Array in Southern California, *Bull. Seism. Soc. Am.* **86,** 306–319.

Tucker, B. E., and J. L. King (1984). Dependence of sediment-filled valley response on input amplitude and valley properties, *Bull. Seism. Soc. Am.* **74,** 153–165.

Venkataraman, A., L. Rivera, and H. Kanamori (2002). Radiated energy from the 16 October 1999 Hector Mine earthquake: regional and teleseismic estimates, *Bull. Seism. Soc. Am.* **92,** 1256–1265.

Zhao, L.-S., and D. V. Helmberger (1994). Source estimation from broadband regional seismograms, *Bull. Seism. Soc. Am.* **84,** no. 1, 91–104.

Zhu, L., and D. V. Helmberger (1996). Advancement in source estimation techniques using broadband regional seismograms, *Bull. Seism. Soc. Am.* **86,** no. 5, 1634–1641.

Istituto Nazionale di Geofisica e Vulcanologia, Rome
Via di Vigna Murata 605
00143 Rome, Italy
malagnini@ingv.it, akinci@ingv.it
(L.M., A.A)

Center for Earthquake Research and Information
University of Memphis
Memphis, Tennessee 38152
bodin@ceri.memphis.edu
(P.B.)

Lawrence Livermore National Laboratory
Ground-Based Nuclear Explosion Monitoring Program
L-205, P.O. Box 808
Livermore, California 94551
mayeda2@llnl.gov
(K.M.)

Manuscript received 2 May 2005.